Title
Molecular Editing of Cellular Responses by the High-Affinity Receptor for IgE

Journal
Science, 343(6174)

ISSN
0036-8075

Authors
Suzuki, Ryo
Leach, Sarah
Liu, Wenhua
et al.

Publication Date
2014-02-28

DOI
10.1126/science.1246976

Peer reviewed

Published in final edited form as:
Science. 2014 February 28; 343(6174): 1021–1025. doi:10.1126/science.1246976.

Molecular Editing of Cellular Responses by the High Affinity Receptor for IgE

Ryo Suzuki[1], **Sarah Leach**[1], **Wenhua Liu**[2], **Evelyn Ralston**[2], **Jörg Scheffel**[1], **Weiguo Zhang**[3], **Clifford A. Lowell**[4], and **Juan Rivera**[1]

[1]Laboratory of Molecular Immunogenetics, National Institute of Arthritis and Musculoskeletal and Skin Diseases, National Institutes of Health, Bethesda, Maryland 20892

[2]Light Imaging Section, Office of Science and Technology, National Institute of Arthritis and Musculoskeletal and Skin Diseases, National Institutes of Health, Bethesda, Maryland 20892

[3]Department of Immunology, Duke University School of Medicine, Durham, North Carolina 27710

[4]Department of Laboratory Medicine, University of California San Francisco, San Francisco, California 94143

Abstract

Cellular responses elicited by cell surface receptors differ depending on stimulus strength. We investigated how the high affinity receptor for IgE modulates the response of mast cells to a high- or low-affinity stimulus. Although both high- and low-affinity stimuli elicited similar receptor phosphorylation; receptor cluster size, mobility, distribution, and the cells' effector responses differed. Low-affinity stimulation increased receptor association with the Src family kinase Fgr, and shifted signals from the adapter LAT1 to the related adapter LAT2. LAT1-dependent calcium signals required for mast cell degranulation were dampened, but the role of LAT2 in chemokine production was enhanced altering immune cell recruitment at the site of inflammation. The findings uncover how receptor discrimination of stimulus strength can be interpreted into distinct *in vivo* outcomes.

It has long been recognized that there are many subtleties in how receptors function to determine a cells' response. For example, vegetative growth of the yeast *Saccharomyces cerevisiae* is elicited by low pheromone concentrations recognized by the pheromone receptor Ste2, whereas intermediate and high pheromone concentrations sensed by this receptor lead to chemotropic growth or mating, respectively (1). Mathematical modeling suggests that yeast translate pheromone concentration as the duration of the transmitted signal (2).

All data are provided in the main paper and supplementary materials.

The authors declare no conflicts of interest.

Supplementary Materials
www.sciencemag.org/cgi/content/full.....
Materials and Methods
Figs S1 to S7
Movies S1 to S3
References

We explored how the high affinity IgE receptor (FcεRI) deciphers high- from low-affinity stimulation to modulate the mast cells' effector responses. Engagement of FcεRI on mast cells and basophils is central to allergic responses (3, 4). Allergic individuals may produce IgE antibodies to offending allergens (a term used for allergy-inducing antigens). These IgE antibodies bind [via their crystallizable fragment (Fc)] to FcεRI with high affinity, with the half-life of IgE bound to FcεRI measured in days (5). Interaction of antigen with FcεRI-bound antigen-specific IgE clusters the individual receptors (6, 7), a step required for generation of intracellular signals that cause mast cells and basophils to release allergic mediators (3, 8). The antigen-binding (Fab) portion of FcεRI-bound IgE antibodies may differ in their affinity for the antigen [as seen in allergic individuals (9)], presumably affecting the duration of the transmitted signal and subsequent outcome. Whether FcεRI functionally distinguishes differences in the affinity of IgE antibody and antigen interactions is not clear. To investigate this, two previously described antigens (10), dinitrophenyl-caproate-Fab (DNP, high affinity) and 2-nitrophenyl-caproate-Fab (2NP, low affinity) were used. These differ in their relative affinities for binding to FcεRI-bound DNP-specific IgE by approximately three orders of magnitude. In bone marrow-derived mouse mast cells (BMMC) (11) FcεRI phosphorylation was similar with approximately 100-fold more 2NP (3000ng/ml) than DNP (30ng/ml) (fig. S1A) and the kinetics of FcεRI phosphorylation were unaltered at these concentrations (fig S1B). However, cellular responses differed as 2NP elicited less than 20% of the DNP-induced degranulation response (fig 1A) at 3000 and 30 ng/ml, respectively, and showed reduced leukotriene B4 (fig 1B) and cytokine production (fig 1C), but enhanced chemokine production (fig 1D). DNP- and 2NP-induced responses required the presence of DNP-specific IgE (fig S2A and B) and 2NP-treatment had no effect on responses initiated through ovalbumin (OVA)-specific IgE (fig S2C and D).

To explore the differences in DNP- and 2NP-induced FcεRI clustering, total internal reflection flourescence (TIRF) microscopy was utilized to study DNP-specific IgE-bearing mast cells after their contact with either a DNP- or 2NP-imbedded planar supported lipid bilayer; while maintaining equal receptor phosphorylation and the differences in mast cell degranulation (figs S3A and B). Exposure to DNP resulted in highly mobile receptor clusters that moved from the cell periphery towards the cell center to form a synapse-like localization as described for the T cell receptor (12, 13) (movie S1A). In contrast, treatment with 2NP revealed slower movement of receptor clusters and a diffuse distribution with a loosely organized synapse-like structure at the cell center (movie S1B). Analysis of receptor cluster movement with time (fig 2A) revealed greater numbers of receptor clusters at the periphery in 2NP-treated cells. The total number of clusters formed at any given time was greater upon DNP-treatment (fig 2B) but the area occupied by these clusters was larger after 2NP-treatment (fig 2C). Relative mobility of receptor clusters in cells treated with 2NP was on average one third that of clusters formed by DNP-treatment (fig 2D). Phospho-tyrosine (a hallmark of intracellular signaling) was localized with both DNP- and 2NP-formed receptor clusters albeit stronger co-localization was evident after 2NP-treatment (fig 2E). The findings demonstrate that the FcεRI clusters induced by DNP or 2NP differ spatiotemporally.

We explored whether differences in the spatiotemporal behavior of receptor clustering by DNP or 2NP were translated into changes in FcεRI-generated intracellular signals. Analysis

of the phosphorylation of FcεRIγ (Y47) showed increased phosphorylation at this site (fig 3A) after cell treatment with 2NP, relative to DNP, and the increased phosphorylation was not dependent on Syk, Fyn, or Lyn; albeit Lyn-deficiency reduced the overall phosphorylation of FcεRI for both stimuli (14). In contrast, phosphorylation of Syk on the activation loop tyrosines (Y519 and Y520), a marker of its activity, was reduced with 2NP treatment (fig S4A). The adapter molecule linker for activation of T cells (LAT)1, is a target of Syk and scaffolds multiple signaling molecules at the plasma membrane including the phospholipases PLCγ1 and PLCγ2, whose activity is essential for initiating release of calcium from intracellular stores. Phosphorylation of LAT1 (fig 3B) and of PLCγ1 and PLCγ2 (fig S4B) was greater in DNP- than in 2NP-treated cells. Calcium mobilization, a key regulator of degranulation (15), from intracellular or extracellular sources was also greater upon DNP-treatment (fig 3C), consistent with the better degranulation of DNP- relative to 2NP-treated cells. Phosphorylation of the LAT1-related adapter, LAT2, was increased (fig 3B) in 2NP-treated mast cells. Greater co-localization of LAT2 with FcεRI was observed in 2NP-treated cells when compared to DNP-treated cells (movies S2A and S2B) and these differences (as determined by flouresence intensity) were quantifiable (fig. 3D). Thus, the differences in FcεRI clustering by DNP or 2NP alter the balance of molecular signaling, dampening some (i.e., LAT1 and PLCγ phosphorylation) but enhancing others (i.e., LAT2 phosphorylation).

Although the absence of Lyn in mast cells caused decreased phosphorylation of FcεRIγ on Y47 (fig 3A), phosphorylation at this site was greater in 2NP-treated cells relative to DNP-treated cells suggesting the possible phosphorylation of FcεRI by another tyrosine kinase after 2NP-treatment. FcεRI phosphorylation was completely inhibited by the Src-family kinase selective inhibitor, 4-Amino-5-(4-chlorophenyl)-7-(*t*-butyl)pyrazolo[3,4-d]pyrimidine (also known as AG1879 or PP2) (fig S5A). Multiple Src family kinases are expressed in mast cells including Fgr, Fyn, Hck, Lyn, and Yes, albeit Yes is seemingly restricted to transformed mast cell lines (16). Hck deficiency in mast cells results in enhanced FcεRI phosphorylation and Fyn does not contribute to FcεRI phosphorylation (17, 18) but recent work suggested that Fgr can associate with FcεRI ((19), fig S5B) and contribute to its function. In mast cells derived from $fgr^{-/-}/hck^{-/-}/lyn^{-/-}$ mice we found no phosphorylation of FcεRI, LAT1, or LAT2 (fig S5C). Reconstitution of these cells with a retrovirus encoding for Hck also failed to restore phosphorylation of the aforementioned molecules. However, retroviral reconstitution with Fgr restored the phosphorylation of FcεRI, LAT1, and LAT2, even in the absence of Lyn. Phosphorylation of LAT2 was increased relative to LAT1 (fig S5C). Localization of FcεRI with Fgr or Lyn in cells reconstituted with both proteins revealed increased co-localization of Fgr in 2NP-treated cells as compared to DNP-treated cells but no significant change in Lyn co-localization with FcεRI (movies S3A and B). The amount of Fgr associated with FcεRI (as determined by flouresence intensity) in 2NP-treated cells was greater than twice that in DNP-treated cells (fig 3E). Thus, differences in FcεRI clustering result in changes in the balance of receptor-associated kinases and subsequent downstream signaling. To determine whether Fgr or LAT2 contributed to the enhanced chemokine response observed after 2NP stimulation we analyzed the chemokine (C-C) ligand (CCL)2 response of Fgr- or LAT2-deficient mast cells after treatment with DNP or 2NP. Fgr- or LAT2-deficiency impaired CCL2 secretion in response to both DNP

and 2NP (fig 3F). Conversely, overexpression of Fgr enhanced production of CCL2 in response to both DNP and 2NP (fig 3F). Fgr- or LAT2-deficiency enhanced 2NP-induced mast cell degranulation (fig S5D) demonstrating a negative regulatory role on this response.

Subtle changes in cell signaling may have consequences *in vivo*. To test this, a passive cutaneous anaphylaxis model (PCA provides a localized assessment of mast cell responses) was employed maintaining the 100 fold greater 2NP to DNP concentration. At 30 min after exposure to DNP or 2NP, vascular permeability as measured by extravasation of Evan's blue dye (see Supplemental Materials and Methods) was significantly higher in DNP- than 2NP-treated mice (fig S6A). Consistent with this result, more mast cells were degranulated in animals treated with DNP. Ear swelling was significantly different 30 min after DNP- or 2NP-treatment but narrowed with time (fig S6B) and the increase in the thickness of the dermis was similar at 3 hrs after stimulation (fig S6C). Immune cell infiltration was similarly increased in animals exposed to DNP or 2NP (fig S6D). By 12 hrs after stimulation, the thickness of the dermis returned to that of control mice (fig S6E) but immune cell infiltrates were still elevated relative to control mice (fig S6F). Given that an inflammatory response was initiated by either DNP or 2NP, we explored the cell types involved. Gr-1^{+}CD$11c^{-}$CD$11b^{+}$ cells were distinguished on the basis of the myeloid marker 7/4 [Ly-6B.2, which is somewhat more highly expressed by recently generated inflammatory macrophages (20)] from neutrophils as marked by Ly-6G (fig 4A). Exposure to DNP caused increased numbers of neutrophils relative to inflammatory macrophages whereas this ratio was reversed in animals treated with 2NP, consistent with the increased secretion of monocyte- or macrophage-attracting chemokines, like CCL2, CCL3 and CCL4, after treatment of mast cells with 2NP (fig 1D). Whole mount immunohistochemical analysis of the skin also revealed these differences (fig 4B and C) and skin mast cells from 2NP-treated mice produced greater amounts of CCL2 than did those in the skin of DNP-treated mice (fig S7). Thus, low affinity stimulation of FcεRI results in an inflammatory response marked by a shift in the monocyte or macrophage:neutrophil ratio.

Collectively, the findings demonstrate that differences in the affinity of antigen and antibody interactions are discriminated by receptors through qualitative changes in molecular signals resulting in distinct outcomes. This discriminatory ability of receptors may extend beyond the immune system.

Supplementary Material

Refer to Web version on PubMed Central for supplementary material.

Acknowledgments

This work was supported by the intramural research program of the National Institute of Arthritis and Musculoskeletal and Skin Diseases (NIAMS) of the National Institutes of Health (NIH). We acknowledge the support of the Laboratory Animal Care and Use Section and the Flow Cytometry Group of the Office of Science and Technology of NIAMS, NIH.

References and Notes

1. Dohlman HG, Thorner JW. Annu Rev Biochem. 2001; 70:703–754. [PubMed: 11395421]

2. Behar M, Hao N, Dohlman HG, Elston TC. PLoS Comput Biol. 2008; 4:e1000197. [PubMed: 18846202]
3. Kinet JP. Annu Rev Immunol. 1999; 17:931–972. [PubMed: 10358778]
4. Galli SJ, Tsai M, Piliponsky AM. Nature. 2008; 454:445–454. [PubMed: 18650915]
5. Isersky C, Rivera J, Mims S, Triche TJ. J Immunol. 1979; 122:1926–1936. [PubMed: 36432]
6. Metzger H. J Immunol. 1992; 149:1477–1487. [PubMed: 1324276]
7. Andrews NL, et al. Immunity. 2009; 31:469–479. [PubMed: 19747859]
8. Blank U, Rivera J. Trends Immunol. 2004; 25:266–273. [PubMed: 15099567]
9. Jackola DR, Pierson-Mullany LK, Liebeler CL, Blumenthal MN, Rosenberg A. Mol Immunol. 2002; 39:367–377. [PubMed: 12220894]
10. Torigoe C, Inman JK, Metzger H. Science. 1998; 281:568–572. [PubMed: 9677201]
11. Razin E. Methods Enzymol. 1990; 187:514–520. [PubMed: 2233359]
12. Monks CR, Freiberg BA, Kupfer H, Sciaky N, Kupfer A. Nature. 1998; 395:82–86. [PubMed: 9738502]
13. Grakoui A, et al. Science. 1999; 285:221–227. [PubMed: 10398592]
14. Parravicini V, et al. Nat Immunol. 2002; 3:741–748. [PubMed: 12089510]
15. Vig M, et al. Nat Immunol. 2008; 9:89–96. [PubMed: 18059270]
16. Gilfillan AM, Rivera J. Immunol Rev. 2009; 228:149–169. [PubMed: 19290926]
17. Hong H, et al. Blood. 2007; 111:2511–2519. [PubMed: 17513616]
18. Gomez G, et al. J Immunol. 2005; 175:7602–7610. [PubMed: 16301670]
19. Lee JH, et al. J Immunol. 2011; 187:1807–1815. [PubMed: 21746961]
20. Rosas M, Thomas B, Stacey M, Gordon S, Taylor PR. J Leukoc Biol. 2010; 88:169–180. [PubMed: 20400676]

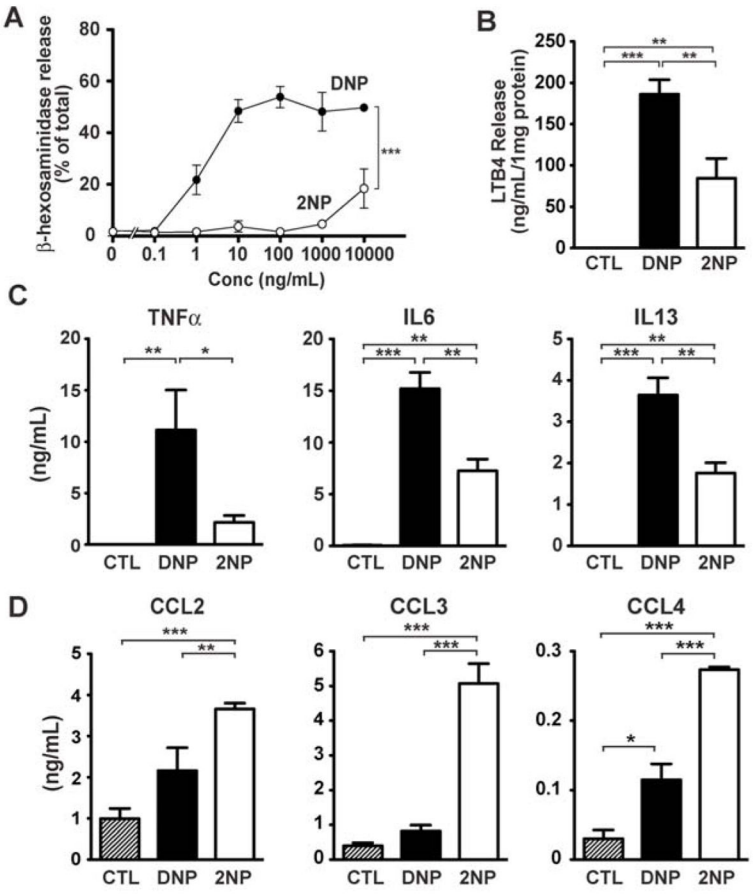

Fig. 1. Mast cell responses differ following DNP- or 2NP-stimulation of FcεRI

(A) Degranulation (as measured by β-hexosaminidase release) of WT BMMCs after stimulation with indicated concentrations of DNP or 2NP. *** p<0.001, two-way ANOVA. **(B)** Leukotriene B_4 (LTB_4) secretion from BMMCs induced by treatment with 3000ng/ml 2NP is less than that with 30 ng/ml of DNP. **p<0.01, *** p<0.001, one-way ANOVA. **(C)** TNFα, IL6 and IL13 are similarly affected at the concentrations of DNP and 2NP indicated in (B). *p<0.05, **p<0.01, *** p<0.001, one-way ANOVA. **(D)** Release of CCL2, CCL3, and CCL4 is increased after stimulation with 2NP relative to DNP (conditions as in B). **p<0.01, *** p<0.001, one-way ANOVA. Data was collected from 4–8 individual experiments.

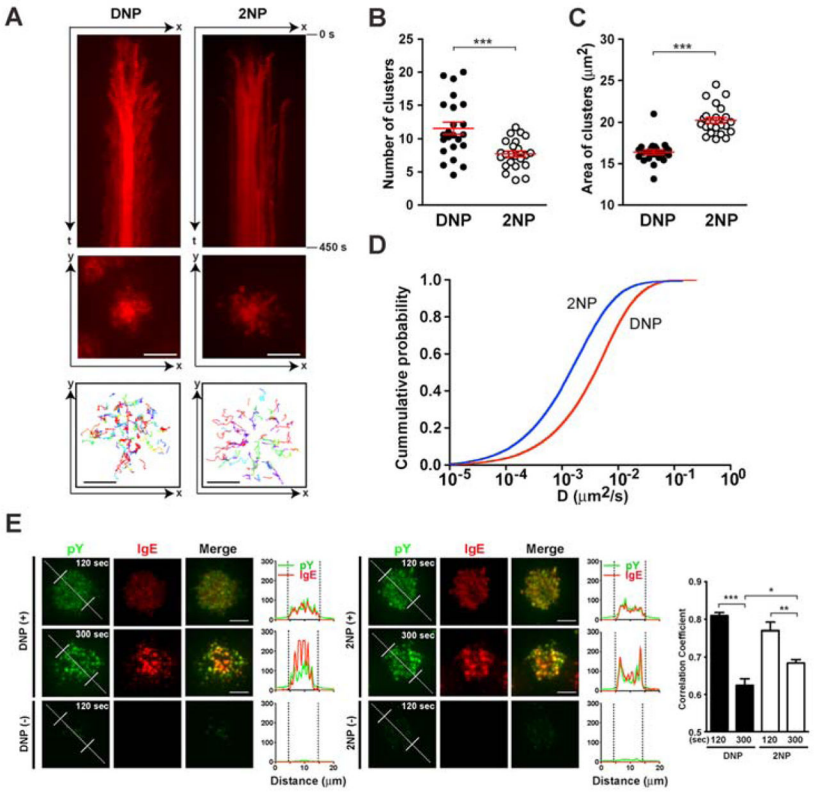

Fig. 2. Characteristics of FcεRI clusters differ with 2NP- or DNP-stimulation of BMMCs

(A) Kymographs of a mast cell labeled with Alexa Fluor 568-labeled IgE (as an FcεRI marker) as captured by TIRF microscopy. Static view of IgE-FcεRI microcluster dynamics (trajectory) captured upon cell contact with DNP or 2NP imbedded in a planar supported lipid bilayer (see Supplemental Materials and Methods) is shown in two dimension (x and y) of movement. Movement of receptors clusters with time (t) is also shown. Sequential image sections for 0.5 to 450 sec are shown in chronological order. Bars = 5 μm. **(B)** The average number of IgE-FcεRI clusters on DNP- or 2NP-imbedded planar supported lipid bilayer is different. Red bars are means ± SE from 24 individual cells. *** $p<0.001$, Student's *t* test. **(C)** Average area of IgE-FcεRI clusters on DNP- or 2NP-imbedded planar supported lipid bilayers differs. Red bars are means ± SE from 24 individual cells. *** $p<0.001$, Student's *t* test. **(D)** Cumulative probability distribution of the diffusion coefficient of individual FcεRI clusters at any given time from analysis of 7835–11198 FcεRI clusters on 24 different cells for DNP and 2NP. **(E)** Tyrosine phosphorylation with IgE-FcεRI microclusters in DNP- or 2NP-treated cells as determined by intracellular staining with antibodies to phosphotyrosine. Fluorescence intensity in cross section (white dotted line) is shown. Localization was analyzed for more than 40 cells in each condition. Bars = 5 μm. * $p<0.05$, ** $p<0.01$, *** $p<0.001$, one-way ANOVA. Data is representative of at least 3 independent experiments.

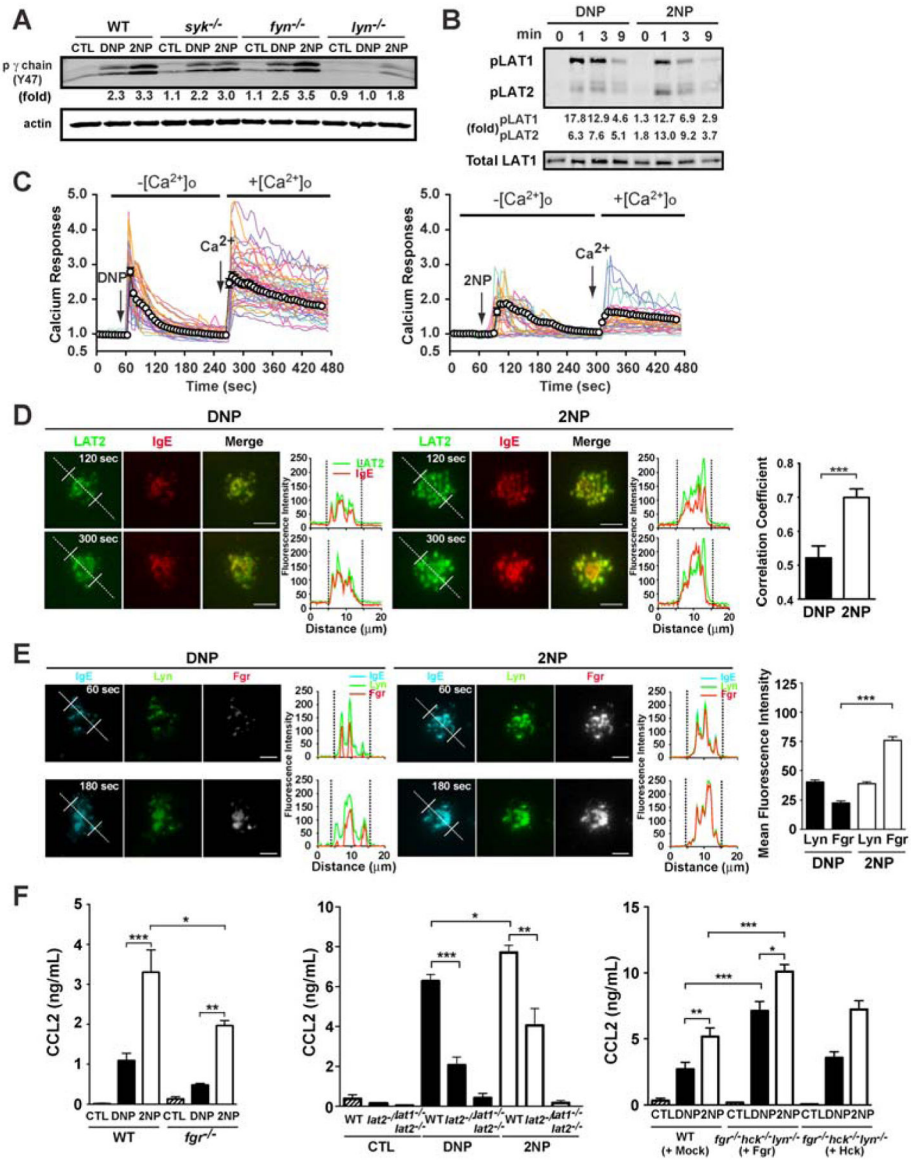

Fig. 3. Distinct molecular signals are induced in 2NP-treated BMMCs: enhanced role for Fgr and LAT2

(A) Phosphorylation of the FcεRI (ITAMγ Y47) in WT, *syk*$^{-/-}$, *fyn*$^{-/-}$, and *lyn*$^{-/-}$ BMMCs after DNP- (30ng/ml) or 2NP- (3000ng/ml) treatment. Fold increase normalized to the control (CTL) for WT. **(B)** Kinetics of LAT1 and LAT2 phosphorylation detected by Western Blot differ in cells treated with DNP or 2NP. Fold increase normalized to DNP (0 min). **(C)** Single cell analysis of BMMC calcium responses in the absence or presence of extracellular Ca (−[Ca^{2+}]o; +[Ca^{2+}]o) as indicated. Fluorescence intensity of a single cell with time (more than 300 cells were monitored in total) was measured and shown as the "calcium response" normalized to the baseline flourescence. Single cells, solid colored lines; averaged responses, black line with open circles. **(D)** Localization of the LAT2-RFP (Green) in *lat2*$^{-/-}$ BMMCs with Alexa Fluor 647-conjugated IgE (Red, marking FcεRI) after DNP- or 2NP-treatment. Images were captured by TIRF microscopy at 120 or 300 sec.

Fluorescence intensities of IgE-FcεRI microclusters and LAT2-RFP are shown in the graphs. Co-localization was analyzed in 15 – 30 cells for each condition. *** $p<0.001$, Student's *t* test. Bar = 5 μm. **(E)** Fluorescence intensities of Lyn-YFP (Green), Fgr-RFP (White), IgE-FcεRI microclusters (Cyan) in BMMCs derived from $fgr^{-/-}hck^{-/-}lyn^{-/-}$ mice treated with DNP or 2NP for 60 or 120 sec. Mean fluorescence intensity was measured from at least 50 cells for each condition. *** $p<0.001$, Student's *t* test. Bar = 5 μm. **(F)** CCL2 secretion by BMMCs from the indicated mice. *$p<0.05$, **$p<0.01$, *** $p<0.001$, one-way ANOVA. Data are a mean ± SE from at least 4 individual experiments.

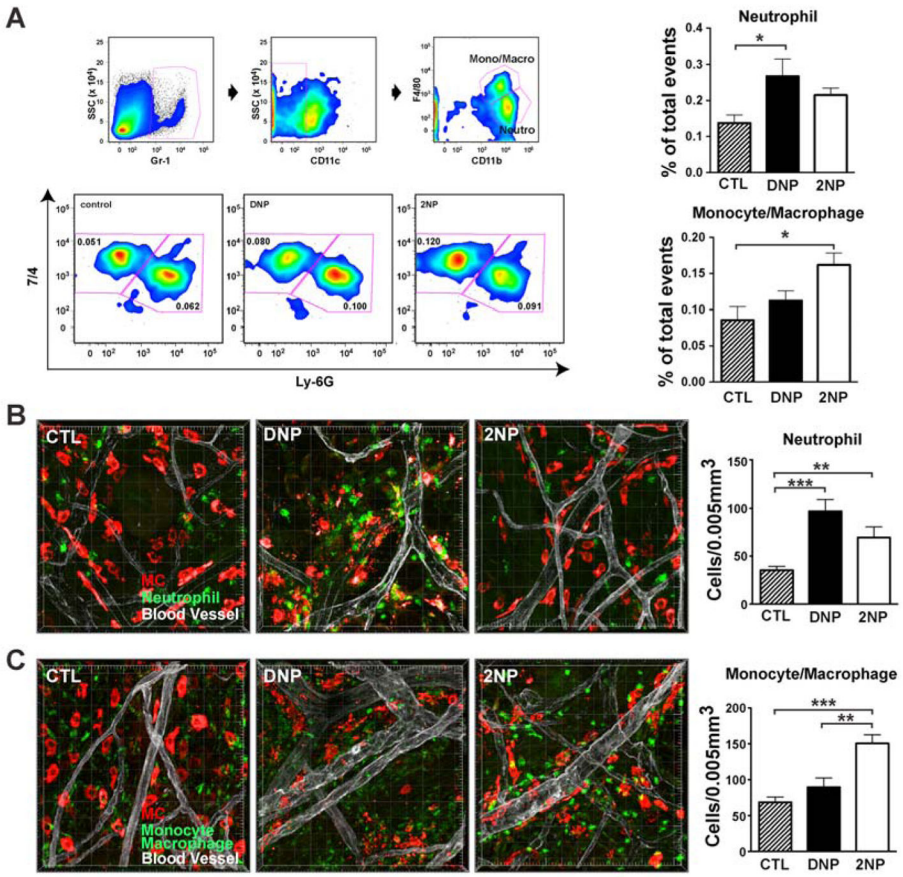

Fig. 4. Immune cell recruitment at the site of inflammation differs in mice treated with DNP or 2NP after passive cutaneous anaphylaxis (PCA)

(A) FACS identifying cell types recruited to the site of inflammation. Monocytes or macrophages and neutrophils were identified as Gr-1^{+} (hi) CD11c^{-} CD11b^{+} F4/80^{+} (intermediate) neutrophil [7/4]$^{+}$ Ly-6G^{-} and Gr-1^{+} (hi) CD11c^{-} CD11b^{+} F4/80^{+} (intermediate) neutrophil [7/4]$^{+}$ Ly-6G^{+}, respectively. Data are mean ± SE from at least 6 individual experiments. $^{*}p < 0.05$, one-way ANOVA. **(B, C)** Whole-mount ear tissue immunostaining after PCA reaction reveals differential immune cell recruitment after DNP- or 2NP-treatment. Mast cells (red) are located along blood vessel (white) and degranulation was observed under DNP challenge (middle panel). Total number of neutrophils (green in B) or monocyte or macrophages (green in C) in random images from 6–8 ears per group were counted and normalized per 0.005mm^3. Data are mean ± SE. $^{**}p < 0.01$, $^{***}p < 0.001$, one-way ANOVA. One representative image of at least 3 independent experiments is shown for (**B**) and (**C**).